Assessing PM2.5 Exposures with High Spatiotemporal Resolution across the Continental United States

Qian Di[†,*], **Itai Kloog**[†,‡], **Petros Koutrakis**[†], **Alexei Lyapustin**[§], **Yujie Wang**[§], and **Joel Schwartz**[†]

[†]Department of Environmental Health, Harvard T.H. Chan School of Public Heath, Boston, MA, 02115, USA

[§]GEST/UMBC, NASA Goddard Space Flight Center, Baltimore, MD, USA

Abstract

A number of models have been developed to estimate $PM_{2.5}$ exposure, including satellite-based aerosol optical depth (AOD) models, land-use regression or chemical transport model simulation, all with both strengths and weaknesses. Variables like normalized difference vegetation index (NDVI), surface reflectance, absorbing aerosol index and meteoroidal fields, are also informative about $PM_{2.5}$ concentrations. Our objective is to establish a hybrid model which incorporates multiple approaches and input variables to improve model performance. To account for complex atmospheric mechanisms, we used a neural network for its capacity to model nonlinearity and interactions. We used convolutional layers, which aggregate neighboring information, into a neural network to account for spatial and temporal autocorrelation. We trained the neural network for the continental United States from 2000 to 2012 and tested it with left out monitors. Ten-fold cross-validation revealed a good model performance with total R^2 of 0.84 on the left out monitors. Regional R^2 could be even higher for the Eastern and Central United States. Model performance was still good at low $PM_{2.5}$ concentrations. Then, we used the trained neural network to make daily prediction of $PM_{2.5}$ at 1 km×1 km grid cells. This model allows epidemiologists to access $PM_{2.5}$ exposure in both the short-term and the long-term.
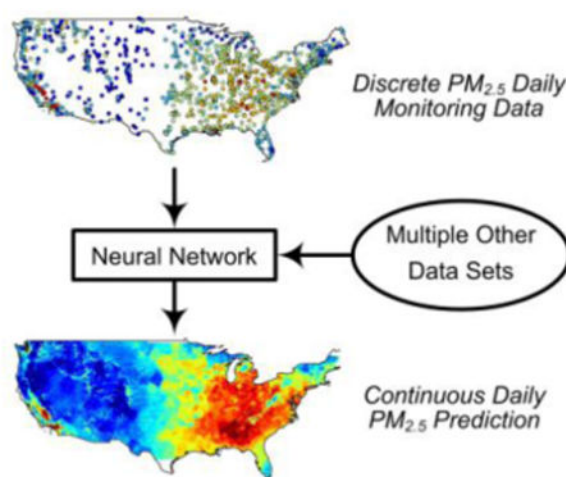
Graphical abstract

---

[*]Corresponding Author: (Q.D.) Phone: 814-777-8202; qiandi@mail.harvard.edu.
[‡]Present Addresses: Department of Geography and Environmental Development, Ben-Gurion University of the Negev, Beer Sheva, P.O.B. 653, Israel

Discrete PM$_{2.5}$ Daily Monitoring Data

Neural Network ← Multiple Other Data Sets

Continuous Daily PM$_{2.5}$ Prediction

Keywords

PM$_{2.5}$; Aerosol optical depth; GEOS-Chem; Absorbing aerosol index; Land-use regression; Convolutional neural network

1. Introduction

Fine particulate matter (PM$_{2.5}$) is a major concern in public health.[1-6] An adverse health effect is associated with PM$_{2.5}$ exposure in the short term[7, 8] and the long term.[9, 10] PM$_{2.5}$ is found to be associated with morbidity,[11, 12] mortality,[6] cardiovascular disease,[4] respiratory disease,[13] myocardial infarction,[14] an increase in hospital admission[11, 15, 16] and others.[17]

Accurate exposure assessment of PM$_{2.5}$ is a prerequisite of to investigate its adverse health effect. Early studies estimated PM$_{2.5}$ at the nearest monitoring station.[18] However, nearest monitors cannot capture all variability in PM$_{2.5}$ concentrations and nondifferential misclassification occurs.[19]

Various approaches have been developed to achieve better exposure assessment. Spatial interpolation, including nearest-neighbor interpolation and Kriging interpolation, was used to smooth PM$_{2.5}$ concentration and estimate local exposure. Nonetheless, interpolation adds no additional information to the model. Local emission like highways between two monitor sites is not captured by simple interpolation. Land-use regression (LUR) uses land-use terms, such as road density, percentage of urban and others, as proxies for PM$_{2.5}$ concentration.[20, 21] Although LUR could achieve a high spatial resolution, it has limited temporal resolution since land-use terms are usually time-invariant.[22] Recent improvements in land-use regression enable incorporation some level of time-variant factors,[23, 24] but land-use terms are still inadequate in modeling short-term variations and often limited by short temporal coverage.[25]

Satellite-based aerosol optical depth (AOD) measurements have been widely used to estimate PM$_{2.5}$ in various models for its large spatial coverage and repeated daily observations.[26] AOD measures the light extinction due to aerosol in the whole atmospheric

column.[27] To obtain ground-level $PM_{2.5}$ concentration, vertical distribution of aerosol is needed. Recent studies proposed different calibration methods.[26, 28-32] Most studies focused on quantifying relationship between AOD and $PM_{2.5}$ or predict a long-term average of $PM_{2.5}$, while epidemiological studies also need short-term $PM_{2.5}$ assessment. Some studies combined AOD and land-use regression and used mixed effect model to achieve improvements on model performance.[33-35] However, the drawback of AOD is missing data, which is caused by bright surfaces or cloud contamination, especially in winter.[36] Also, AOD measurements may also have abnormally large values caused by forest fires.[37] For grid cells with missing or abnormal values, the AOD-$PM_{2.5}$ relationship may be problematic, especially for daily $PM_{2.5}$ assessment. The relationship between column aerosol concentration and ground-level concentration can be influenced by multiple factors such as meteorological fields, chemical profile of aerosol, and others.[38, 39] The absorbing aerosol index (AAI) provides information about aerosol type and is informative to $PM_{2.5}$ modeling.[40, 41]

Chemical transport models (CTMs), like GEOS-Chem,[42] CMAQ,[43] and CHIMERE,[44] simulate the formation, dispersion and deposition of fine particles based on emission inventories and known atmospheric chemical reaction. CTM is another way to assess $PM_{2.5}$ concentration. Due to the complexity of reactions and atmospheric meteorological processes, simulated concentration often deviates from the real world. CTM outputs are often used after calibration.[45, 46] CTM provides an aerosol vertical profile, which has been used as scaling factor in AOD calibration.[29, 47] Due to the limit of computation, CTM usually has coarse spatial resolution. In a previous study, we have proposed a hybrid model which uses land-use regression to downscale CTM outputs.[48]

Existing approaches have both strengths and weaknesses, and often they complement to each other. In this paper, we incorporated multiple variables into a neural network-based hybrid model, including satellite-based AOD data, AAI, CTM outputs, land-use terms, and meteorological variables. We validated the model with 10-fold cross-validation and predicted daily $PM_{2.5}$ at 1 km×1 km resolution in the continental United States for the years 2000-2012. Prediction with such a high temporal and spatial resolution allows epidemiological studies to estimate health effect of $PM_{2.5}$ with greater reliability.

2. Materials

2.1. Study Domain

The study domain is the continental United States, including 48 contiguous states and Washington, D.C (Figure S1). The study period is from January 1st, 2000 to December 31st, 2012, a total of 4,749 days.

2.2. Monitoring Data

Monitoring data for $PM_{2.5}$ were collected by EPA Air Quality System (AQS). In total, there were 1,986 monitor stations available in this period and 1,928 of them were located in the study area. Not every monitoring site has data available throughout the study period. Monitoring sites were densely distributed along coastal areas and the Eastern part, while

there were a few monitors in the Mountain Region (Figure S1). We calibrated our hybrid model to the daily average of monitored PM$_{2.5}$.

2.3. AOD Data

The Moderate Resolution Imaging Spectroradiometer (MODIS) is an instrument aboard the Earth Observing System (EOS) satellite.[49, 50] Several algorithms have been developed to retrieve AOD data from MODIS measurement,[51] including a recent algorithm called MAIAC, which retrieves AOD with a spatial resolution of 1 km×1 km.[52-54] We used MAIAC AOD data from Aqua satellite from 2003 to 2012 and Terra satellite from 2001 to 2012. The MAIAC algorithm arranges data at 600 km×600 km tile, which includes 360,000 1 km×1 km grid cells. In total 33 tiles and 11,880,000 grid cells were used in this study, which is also the grid cell we made predictions at. Grid cells over water bodies were excluded from the study.

AOD data has some portion of missing values, especially in the winter. Missing values are caused by bright surfaces (e.g. snow coverage) and cloud contamination.[36] In addition, AOD data may have abnormally large values due to extreme events like forest fires.[37] Usually AOD data with values above 1.5 are excluded from modeling, which also creates missing values.[55] Our previous study calibrated column aerosol mass from CTM outputs to satellite-based AOD and predicted AOD values when satellite-based AOD are missing.[56] For AOD data used in this study, we filled in the missing values using this method as preprocessing (Section 3, Supplementary Material).

2.4. Surface Reflectance

Surface characteristics and errors in AOD data products have been well documented by previous studies.[57] The MAIAC algorithm was designed to retrieve AOD over various surfaces, but surface brightness can still affect data quality.[54] We used MODIS surface reflectance data (MOD09A1) to control for that.[58] MOD13A1 has a spatial resolution of 500 m×500 m and a temporal resolution of 8 days. We used surface reflectance from Band 3 and linearly interpolated values for days without measurements.

2.5. Chemical Transport Model Outputs

We used GEOS-Chem, a chemical transport model, to simulate ground-level PM$_{2.5}$ concentration. GEOS-Chem is a global 3-dimensional chemical transport model, which uses meteorological inputs and emission inventories to simulate atmospheric components. The details of GEOS-Chem is articulated somewhere else.[42] We performed a nested grid simulation (Version 9.0.2) for North America at 0.500°×0.667° from 2005 to 2012, with boundary conditions exported from a 2.0°×2.5° global simulation. Since meteorological inputs at 0.500°×0.667° are not available from 2000 to 2004, we used 2.0°×2.5° outputs instead. Based on previous studies and pilot testing, total PM$_{2.5}$ was defined as the sum of nitrate, sulfate, elemental carbon, organic carbon, ammonium, sea salt aerosol, dust aerosol and others (Table S2).[59]

In additional to providing ground-level PM$_{2.5}$ estimation, GEOS-Chem also simulates vertical distribution of aerosol, which could be used for calibrating AOD. Previous studies

used GEOS-Chem to compute the percentage of ground-level aerosol in the total column aerosol. This percentage was used in AOD calibration as a scaling factor.[29, 60] Both studies utilized GEOS-Chem to provide both direct estimation for ground-level $PM_{2.5}$ and a scaling factor to calibrate AOD.

2.6. Meteorological Data

Meteorological fields were obtained from NCEP North American Regional Reanalysis data, which assimilates various data sources like land-surface, ship, radiosonde, pibal, aircraft, satellite and others.[61] Meteorological data are daily estimate at 0.3° grid cells (about 32 km). In total 16 meteorological variables were used in this study. They include air temperature, accumulated total precipitation, downward shortwave radiation flux, accumulated total evaporation, planetary boundary layer height, low cloud area fraction, precipitable water for the entire atmosphere, pressure, specific humidity at 2m, visibility, wind speed, medium cloud area fraction, high cloud area fraction, and albedo. Wind speed was computed as the vector sum of u-wind (east-west component of the wind) at 10m and v-wind (north-south component) at 10m.

2.7. Aerosol Index Data

Absorbing aerosol index (AAI) indicates the presence of absorbing aerosols in the atmosphere. Major sources of absorbing aerosol include biomass burning and desert dust; other minor sources could be volcanic ash.[62] AAI is informative for estimating absorbing aerosols, such as organic carbon and soil dust.[63, 64] We used AAI Level 3 data products from the Ozone Monitoring Instrument (OMI), where two algorithms are used in retrieval. One is a near-UV algorithm, which retrieves UV aerosol index (OMI data product OMAERUVd);[62, 64] and the other one uses multiwavelength aerosol algorithm, whose outputs include aerosol indexes at visible and UV range (OMI data product OMAEROe).[65] Both algorithms have pros and cons, which have been discussed previously.[66] Both data products are complementary, and thus we used both. OMI AAI data is available after October 2004. OMAERUVd data product has a spatial resolution of 1°; OMAEROe data product has a spatial resolution of 0.25°.

2.8. Land-use terms

Land-use terms serve as proxies for emissions and are used to capture variations at a small a spatial scale, which may not modeled by GEOS-Chem. The detailed process of obtaining land-terms like elevation, road density, NEI (National Emissions Inventory) emission inventory, population density, percentage of urban, and NDVI has been reported somewhere else.[67] For vegetation coverage, we used percentage of vegetation from NCEP North American Regional Reanalysis data and MODIS MOD13A2, a NDVI data product.[68] MOD13A2 has a spatial resolution of 1 km×1 km and a temporal resolution of 16 days. We linearly interpolated NDVI values for days without measurements.

2.9. Regional and Monthly Dummy

Previous studies found the relationship between AOD and $PM_{2.5}$ have regional and daily variation due to the difference in meteorology and aerosol composition.[38, 69] Atmospheric

mechanism is complex, and relationships between other variables could also differ temporally and spatially. To account for that, we used monthly and regional dummy variables. Regional dummy variable comes from major climate types in the United States (Figure S3).[70] Since the AOD-PM$_{2.5}$ relationship can change from day to day, daily dummy variables would be ideal. However, training a neural network with 365 indicator variables in addition to the other variables would be computationally intensive, and we used monthly dummy variables as a compromise.

3. Methods

We trained a neural network with the above variables to PM$_{2.5}$ monitoring data from the AQS network. The relationships between input variables and PM$_{2.5}$ could be highly nonlinear with complex interactions. Neural networks have the potential to model any type of nonlinearity.[71, 72] The details of the neural network, such as its structure and training method were articulated in the supplementary material. All input variables covered the entire study area, but some of them were not available in early years or had higher proportions of missing values. Missing values were especially common in Terra and Aqua AOD data. To deal with the missing values problem and different temporal coverages, we adopted the following steps. We used a calibration method to fill in the missing values in Aqua AOD data from 2003 to 2012 and Terra AOD data from 2001 to 2012 based on the association of GEOS-Chem outputs and land-use terms with non-missing AOD.[56] For the other variables with a low fraction of missing values, we interpolated at grid cells with missing values. Regarding temporal coverage, GEOS-Chem outputs, land-use terms, MODIS outputs, and meteorological variables were available throughout the study period. OMI data, Aqua AOD, and Terra AOD were unavailable in earlier years. For years with one or more unavailable variables, we fitted the model with the remaining available variables.

Most previous studies used only *in situ* variables for modeling. However, information from a neighboring cell can be informative as well. For example, nearby road density, forest coverage and other land-use variables as well as nearby PM$_{2.5}$ measurements either influence or correlate with local PM$_{2.5}$ measurements. They are informative for modeling and can improve model performance. We accounted for spatial correlation by using convolutional layers in the neural network.[73] A convolutional layer is computed by applying a convolution kernel on an input layer. Values from neighboring cells are combined through the use of the kernel function. The kernel takes the form a function (e.g. weighted average with Gaussian weights based on distance) that produces a scalar estimate from the multidimensional inputs. A convolution layer aggregates nearby information and can simulate some form of autocorrelation. We included convolutional layers for land-use terms and nearby PM$_{2.5}$ measurements as additional predictor variables to account for spatial autocorrelation. Multiple convolution layers were incorporated to allow the neural network to model even more complex autocorrelation or possible interaction with other variables (Supplementary material). In addition to nearby grid cells, observations from nearby days for the same grid cell can be also informative. To incorporate this, we first fitted a neural network and obtained an initial prediction for PM$_{2.5}$. We then computed temporal convolution layers and fitted the neural network again with them (Figure S5).

To validate model results and avoid overfitting, we used 10-fold cross-validation, in which all monitoring sites were randomly divided into 10%-90% splits. The model was trained with 90% of data and predicted $PM_{2.5}$ at the remaining 10%. The same process was repeated for other splits. Assembling predicted $PM_{2.5}$ at ten 10% testing sets yielded predicted $PM_{2.5}$ for all the monitors. We computed correlation between predicted $PM_{2.5}$ and monitored $PM_{2.5}$. Spatial and temporal R^2s were also calculated. Details of calculating R^2 have been specified in the supplementary material.

The trained neural network was then used to make daily$PM_{2.5}$ predictions for each gridcell (1 km×1 km) for each day.

All programming was implemented in Matlab (version 2014a, The MathWorks, Inc.).

4. Results

To determine input variables, we compared models with different combinations of input variables based on cross-validated total R^2. Model comparison indicated that (1) a hybrid model performed better than any subset models (Figure S6); (2) scaling factor was better to be incorporated as a separate input layer (Figure S7); (3) convolutional layers for land-use variables and predicted $PM_{2.5}$ both improved model performance (Figures S6, S8). Hence, input variables for the final model were GEOS-Chem outputs, Aqua and Terra AOD, scaling factor, OMI AAIs, meteorological variables, NDVI, surface reflectance, land-use terms, convolutional layers, and regional/monthly dummy variables. Table 1 presents model performance after conducting 10-fold cross-validation. Total R^2 between fitted and monitored $PM_{2.5}$ ranged from 0.74 to 0.88 and spatial R^2 was from 0.78 to 0.88. By season, the model usually performed better in summer, followed by autumn, spring, and winter (Table S3). By region, regions in the Eastern United States had the best model performance, followed by the Central United States. The Pacific and Mountain regions had a less satisfying model performance. We also found R^2 remained high before 2008 and dropped after 2010 for sub-regions and the whole study area (Table S4). We will discuss possible reasons later. Region name and division are from U.S. census division (Table S1, Figure S2). In terms of spatial pattern, we found an east-west gradient with model performing better in the Eastern and Central United States but less satisfying in the western coast and the Mountain Region (Figure 1). Besides, some areas in the Mountain Region (e.g. Great Basin and Colorado Plateau) with large variability in elevation and surface type have relative low R^2 all the year round. Even in the Eastern United States, where model performance is high in general, areas along Appalachian Mountains and around Ozark Plateau have less satisfying model performance.

Figure 2 shows the spatial distribution of total $PM_{2.5}$ in the study area. The Eastern United States generally had higher $PM_{2.5}$ levels than the Western part. The area around Illinois and Ohio, areas around New York City and Philadelphia, and parts of the Southeastern United States witnessed the heaviest $PM_{2.5}$ pollutions in the study area, especially in summer. The San Joaquin Valley, Salt Lake City, and Denver stood out in the Western United States for their high $PM_{2.5}$ levels. Regarding the temporal trend, the national average dropped from 9.2 μg/m^3 in 2003 to 7.5 μg/m^3 2012 (Figure 3). By regions, the declining trend was

predominantly in the Eastern United States, with largest reduction occurring in East South Central Region (5.8 μg/m^3).

One additional way to validate our exposure estimates is to see if they can reproduce the spatial autocorrelation in PM$_{2.5}$ concentrations. To do this, we calculated the correlation among all pairs of PM$_{2.5}$ monitors in the EPA network, and plotted them as a function of distance. We compared that to the same plot, but using our predicted PM$_{2.5}$ concentrations instead (Figure 4). The results show essential identical trends and substantial overlap between the correlations of actual vs modeled PM$_{2.5}$ with distance.

5. Discussion

Our hybrid model incorporated existing PM$_{2.5}$ models as well as multiple variables and achieved high out-of-sample R^2,averaging 0.84 (0.74~0.88 by year) over the study period. The model performed better in some eastern regions, with an average out of sample R^2 of 0.86~0.89 by region. To our best knowledge, our model performance surpasses existing similar studies. Meanwhile, we predicted PM$_{2.5}$ daily concentrations at nationwide 1 km×1 km grid cells from 2000 to 2012. As discussed below, this level of resolution and coverage is an improvement over current PM$_{2.5}$ models and could be beneficial to epidemiological studies. Epidemiologists could identify long-term and short-term exposure of PM$_{2.5}$ in the whole continental United States at individual level, which helps study adverse health effect of PM$_{2.5}$ with higher accuracy.

There are several advantages and innovations in our approach. First of all, our model covered the whole United States with a spatial resolution of 1 km×1 km and a temporal resolution of 1 day and achieved high R^2. As far as we know, if taking coverage, resolution and model performance into consideration, our model performs better than existing models. As mentioned in the Introduction, most PM$_{2.5}$ modeling work that used AOD data focused on the AOD-PM$_{2.5}$ relationship, instead of making predictions. For studies with a similar research goal as ours, some of them have done AOD calibration at global scale, but their estimation was long-term average[29] or annual average, with some degree of bias (slope=0.68) and modest R^2 (R^2=0.65).[47] A previous study calibrated AOD to daily monitored PM$_{2.5}$ in the Northeastern United States using a mixed model and achieved R^2 around 0.725~0.904.[31] A similar study used the similar method for the Southeastern United States and achieved R^2 around 0.63 to 0.85.[32] Compared with both regional models, our hybrid nationwide model performs slightly better in the Northeastern United States and much better in the Southeastern United States (Table S6). One reason is that aerosol formation in the Southeastern United States is affected by biogenic isoprene emission from trees;[74] while isoprene emission from trees in the Northeastern United States is less of a concern. Secondary organic aerosol that results from isoprene has different absorption than other PM$_{2.5}$ components,[75] which is not well captured by AOD. AAI provides some information about absorption profile, which helps our hybrid model perform much better in the Southeast and almost the same or a little better in the Northeast.

Second, our hybrid model integrated most variables that are known to be informative to PM$_{2.5}$ modeling and improved model performance. This study reminds the importance of

hybrid framework and also proposes a possible neural network-based approach to implement that. Atmospheric mechanism is complex, and a single variable can only capture an incomplete picture. For example, AOD measures the light extinction due to aerosol in the whole atmosphere column. Different aerosols vary in terms of aerosol absorption, which can affect AOD. More complexly, even the same aerosol type could have various absorptions under different meteorological conditions and emission features.[39] This discovery suggests that when modeling $PM_{2.5}$ with AOD data, AAI (proxy for aerosol type), meteorological fields, and emission profiles are also necessary. There could be many unknown mechanisms intertwining with other variables. Multiple variables are not redundant but complementary, which can recover the original picture of atmospheric process and improve model performance to the best.

Third, we used a convolutional layer in the neural network for $PM_{2.5}$ modeling, which is an innovation of our study. Primarily used in computer science, a convolutional kernel is placed over nearby pixels to produce a convolutional layer. Similarly, we used convolutional layers in exposure assessment to aggregate variable values from nearby grid cells or monitoring sites. Previous studies incorporated nearby information by using nearby monitoring measurements, nearby road density, or others, which were all prespecified. Our hybrid model takes multiple convolutional layers, which stand for various ways of aggregating nearby information, and lets learning algorithm decide their relative importance in the model. This approach is versatile and is able to model different neighboring influences, as well as potential interactions with other variables.

Last but not least, we used AOD data with missing values been filled by some calibration model. No further processing is required to deal with missing AOD data, which could have been lengthy and cumbersome in previous studies.

For the east-west gradient in model performance (Figure 1), previous studies also reported that correlation between MODIS AOD and ground-measured $PM_{2.5}$ is better in the eastern part but poor in the western part, and they attributed poor model performance to relative low $PM_{2.5}$ level and variability of terrain.[31, 41] This study lends support to both statements. We quantified the relationship between model performance and elevation at each monitoring site and found a negative correlation despite of much noise (Figure S10). Similarly, a positive association exists between $PM_{2.5}$ level and model performance (Figure S10), which implies that the drop of model performance after 2010 is probably caused by substantive reduction in $PM_{2.5}$ level after 2010. This is also the reason why the Mountain region, with low $PM_{2.5}$ level, has poor model performance. A lower level of $PM_{2.5}$ means a lower signal-to-noise ratio, and model performance drops as model uncertainty keeps constant. Besides, the reduction of sulfate is mainly responsible for decreasing the $PM_{2.5}$ level. Sulfate is better modeled in GEOS-Chem than other major components like nitrate and ammonium,[76] so dropping sulfate causes unsatisfying model performance. For the same reason, we saw a less satisfying model performance in California despite its high $PM_{2.5}$ level, for the reason that California has a high amount of nitrate originated from vehicle exhaust compared with the Eastern United States. This argument suggests that it would be informative to include sulfate in $PM_{2.5}$ modeling work in the future.

Our model performance is still good even at low $PM_{2.5}$ levels. To prove that, we fitted a spline regression of prediction $PM_{2.5}$ to measured $PM_{2.5}$. Linearity between measured and predicted $PM_{2.5}$ holds when $PM_{2.5}$ level is below 70 μg/m^3 and become less obvious above 80 μg/m^3 due to insufficient measurements (Figure 5). Bias at high concentration is less of our concern, since there are few days with the $PM_{2.5}$ level above 80 μg/m^3 in the study area. If constraining to monitored $PM_{2.5}$ below 35 μg/m^3, the EPA daily standard for $PM_{2.5}$, our hybrid model performed even better. Mean R^2 increased to 0.85; slope is close 1; and intercept is close to 0 (Table S5). Good model performance at low $PM_{2.5}$ concentrations enables epidemiologists to estimate the adverse effect of $PM_{2.5}$ even below EPA daily standard.

Figure 2 visualizes the spatial distribution of annual and seasonal average of $PM_{2.5}$. There is also an east-west gradient of the $PM_{2.5}$ level. The Eastern and Central United States suffered relatively heavy $PM_{2.5}$ pollutions, except for the Appalachian Mountains, the Florida Peninsula, and some remote areas in the Northeast. The Southeastern United States, especially Alabama and Georgia, witnessed a high $PM_{2.5}$ level in summer and less noticeably in spring and autumn, which results from isoprene emission from trees. Isoprene emission from trees increases with temperature[74, 77] and peaks in hot summer.[78] The Western United States had relatively low $PM_{2.5}$ levels, but the San Joaquin Valley, Salt Lake City, and Denver stood out for their abnormally high $PM_{2.5}$ level, which was also featured by clear seasonality and a high $PM_{2.5}$ level in winter. This is caused by temperature inversion in winter which prevents atmospheric convection and trapped air pollution near the surface. For temporal trend, the Eastern and Central United States witnessed a decreasing trend in the $PM_{2.5}$ level (Figure 3), which is caused by the reduction of sulfur dioxide from power plant emission. For seasonal cycle, $PM_{2.5}$ level peaks in summer in the Eastern and Central United States due to long-term transported sulfate from power plants and isoprene-related organic carbon. The winter peaks are probably caused by increased fuel burning for heat and local temperature inversion that prevents pollution dispersion.

Exposure assessments are essential for epidemiological studies. The traditional method of exposure assessment relies on nearest monitors, which constraints the number of available participants and introduces measurement errors. Besides, monitoring data from some monitors are intermittent. Our $PM_{2.5}$ predictions have temporal resolution of 1 day and spatial resolution of 1 km×1 km, which lifts the above limitations. Besides, our hybrid model performs still well at low concentrations. Linearity between predicted and monitored $PM_{2.5}$ still holds at low concentrations, without any signal of bias (Figure 5). Cross-validated R^2 indicates a good fit when daily $PM_{2.5}$ level is below 35 μg/m^3 (Table S5), which enable epidemiologists to assess the adverse effect of $PM_{2.5}$ even below the EPA standard. In the long term, there is little discrepancy between long-term averages of predicted and monitored $PM_{2.5}$, with difference below 1 μg/m^3 (Figure S9).

Some limitations remain. Our model requires quite a lot of variables, which limits the application in other countries. This data-intensive approach could be difficulty in other regions where public data is sparse. For regions with less data available, we might have to make a tradeoff between model performance and resolution. For example, instead of daily prediction $PM_{2.5}$ at 1 km×1 km, we may model annual average of $PM_{2.5}$ or at coarse spatial

resolution. Besides, the chemical profile of $PM_{2.5}$ is not available in this framework. Previous epidemiological studies suggest various toxicities of $PM_{2.5}$ chemical components,[79, 80] which is worthy of further investigation.

Supplementary Material

Refer to Web version on PubMed Central for supplementary material.

Acknowledgments

References

1. Lim SS, Vos T, Flaxman AD, Danaei G, Shibuya K, Adair-Rohani H, Al Mazroa MA, Amann M, Anderson HR, Andrews KG. A comparative risk assessment of burden of disease and injury attributable to 67 risk factors and risk factor clusters in 21 regions, 1990–2010: a systematic analysis for the Global Burden of Disease Study 2010. The lancet. 2013; 380(9859):2224–2260.

2. Slama R, Morgenstern V, Cyrys J, Zutavern A, Herbarth O, Wichmann HE, Heinrich J, Group LS. Traffic-related atmospheric pollutants levels during pregnancy and offspring's term birth weight: a study relying on a land-use regression exposure model. Environ Health Persp. 2007:1283–1292.

3. Franklin M, Zeka A, Schwartz J. Association between $PM_{2.5}$ and all-cause and specific-cause mortality in 27 US communities. J Expo Sci Env Epid. 2007; 17(3):279–287.

4. Dominici F, Peng RD, Bell ML, Pham L, McDermott A, Zeger SL, Samet JM. Fine particulate air pollution and hospital admission for cardiovascular and respiratory diseases. Jama. 2006; 295(10): 1127–1134. [PubMed: 16522832]

5. Gent JF, Triche EW, Holford TR, Belanger K, Bracken MB, Beckett WS, Leaderer BP. Association of low-level ozone and fine particles with respiratory symptoms in children with asthma. Jama. 2003; 290(14):1859–1867. [PubMed: 14532314]

6. Schwartz J, Dockery DW, Neas LM. Is daily mortality associated specifically with fine particles? J Air Waste Manage (1995). 1996; 46:927–939.

7. Halonen JI, Lanki T, Yli-Tuomi T, Kulmala M, Tiittanen P, Pekkanen J. Urban air pollution and asthma and COPD hospital emergency room visits. Thorax. 2008

8. Zanobetti A, Schwartz J. The effect of fine and coarse particulate air pollution on mortality: a national analysis. Environ Health Perspect. 2009; 117:898–903. [PubMed: 19590680]

9. Boldo E, Medina S, Le Tertre A, Hurley F, Mücke HG, Ballester F, Aguilera I. Apheis: Health impact assessment of long-term exposure to $PM_{2.5}$ in 23 European cities. Eur J Epidemiol. 2006; 21(6):449–458. [PubMed: 16826453]

10. Schwartz J. Harvesting and long term exposure effects in the relation between air pollution and mortality. Am J Epidemiol. 2000; 151:440–448. [PubMed: 10707911]

11. Lippmann M, Ito K, Nadas A, Burnett R. Association of particulate matter components with daily mortality and morbidity in urban populations. Res Rep HEI. 2000; (95):5–72. discussion 73-82.

12. Sarnat JA, Marmur A, Klein M, Kim E, Russell AG, Sarnat SE, Mulholland JA, Hopke PK, Tolbert PE. Fine particle sources and cardiorespiratory morbidity: an application of chemical mass balance and factor analytical source-apportionment methods. Environ Health Persp. 2008; 116(4):459.

13. Peng RD, Bell ML, Geyh AS, McDermott A, Zeger SL, Samet JM, Dominici F. Emergency Admissions for Cardiovascular and Respiratory Diseases and the Chemical Composition of Fine Particle Air Pollution. Environ Health Persp. 2009; 117:957–963.

14. Peters A, Dockery DW, Muller JE, Mittleman MA. Increased Particulate Air Pollution and the Triggering of Myocardial Infarction. Circulation. 2001; 103:2810–2815. [PubMed: 11401937]

15. Schwartz J. Air pollution and hospital admissions for cardiovascular disease in Tucson. Epidemiology. 1997:371–377. [PubMed: 9209849]

16. Schwartz J, Morris R. Air pollution and hospital admissions for cardiovascular disease in Detroit, Michigan. Am J Epidemiol. 1995; 142(1):23–35. [PubMed: 7785670]

17. Pope CA, Dockery DW. Health Effects of Fine Particulate Air Pollution: Lines that Connect. J Air Waste Manage. 2006; 56:709–742.

18. Laden F, Schwartz J, Speizer FE, Dockery DW. Reduction in fine particulate air pollution and mortality: extended follow-up of the Harvard Six Cities study. Am J Resp Crit Care. 2006; 173:667–672.

19. Pinto JP, Lefohn AS, Shadwick DS. Spatial variability of $PM_{2.5}$ in urban areas in the United States. J Air Waste Manage. 2004; 54(4):440–449.

20. Beckerman BS, Jerrett M, Martin RV, van Donkelaar A, Ross Z, Burnett RT. Application of the deletion/substitution/addition algorithm to selecting land use regression models for interpolating air pollution measurements in California. Atmos Environ. 2013; 77:172–177.

21. Vienneau D, De Hoogh K, Beelen R, Fischer P, Hoek G, Briggs D. Comparison of land-use regression models between Great Britain and the Netherlands. Atmos Environ. 2010; 44(5):688–696.

22. Aguilera I, Sunyer J, Fernández-Patier R, Hoek G, Aguirre-Alfaro A, Meliefste K, Bomboi-Mingarro MT, Nieuwenhuijsen MJ, Herce-Garraleta D, Brunekreef B. Estimation of Outdoor NO_x, NO_2, and BTEX Exposure in a Cohort of Pregnant Women Using Land Use Regression Modeling. Environ Sci Technol. 2008; 42:815–821. [PubMed: 18323107]

23. Ghassoun Y, Ruths M, Löwner MO, Weber S. Intra-urban variation of ultrafine particles as evaluated by process related land use and pollutant driven regression modelling. Science of the Total Environment. 2015; 536:150–160. [PubMed: 26204051]

24. Patton AP, Zamore W, Naumova EN, Levy JI, Brugge D, Durant JL. Transferability and generalizability of regression models of ultrafine particles in urban neighborhoods in the Boston area. Environmental science & technology. 2015; 49(10):6051–6060. [PubMed: 25867675]

25. Hoek G, Beelen R, de Hoogh K, Vienneau D, Gulliver J, Fischer P, Briggs D. A review of land-use regression models to assess spatial variation of outdoor air pollution. Atmospheric Environment. 2008; 42:7561–7578.

26. Streets DG, Canty T, Carmichael GR, de Foy B, Dickerson RR, Duncan BN, Edwards DP, Haynes JA, Henze DK, Houyoux MR. Emissions estimation from satellite retrievals: A review of current capability. Atmos Environ. 2013; 77:1011–1042.

27. Morain, SA., Budge, AM. Environmental Tracking for Public Health Surveillance. CRC Press; 2012.

28. Chu DA, Kaufman Y, Zibordi G, Chern J, Mao J, Li C, Holben B. Global monitoring of air pollution over land from the Earth Observing System-Terra Moderate Resolution Imaging Spectroradiometer (MODIS). J Geophys Res Atoms (1984–2012). 2003; 108(D21)

29. van Donkelaar A, Martin RV, Brauer M, Kahn R, Levy R, Verduzco C, Villeneuve PJ. Global Estimates of Ambient Fine Particulate Matter Concentrations from Satellite-Based Aerosol Optical Depth: Development and Application. Environ Health Persp. 2010; 118:847–855.

30. Van Donkelaar A, Martin RV, Park RJ. Estimating ground-level $PM_{2.5}$ using aerosol optical depth determined from satellite remote sensing. J Geophys Res Atoms (1984–2012). 2006; 111(D21)

31. Engel-Cox JA, Holloman CH, Coutant BW, Hoff RM. Qualitative and quantitative evaluation of MODIS satellite sensor data for regional and urban scale air quality. Atmos Environ. 2004; 38(16):2495–2509.

32. Wang J, Christopher SA. Intercomparison between satellite-derived aerosol optical thickness and $PM_{2.5}$ mass: implications for air quality studies. Geophys Res Lett. 2003; 30(21)

33. Kloog I, Chudnovsky AA, Just AC, Nordio F, Koutrakis P, Coull BA, Lyapustin A, Wang Y, Schwartz J. A new hybrid spatio-temporal model for estimating daily multi-year $PM_{2.5}$ concentrations across northeastern USA using high resolution aerosol optical depth data. Atmos Environ. 2014; 95:581–590.

34. Kloog I, Koutrakis P, Coull BA, Lee HJ, Schwartz J. Assessing temporally and spatially resolved $PM_{2.5}$ exposures for epidemiological studies using satellite aerosol optical depth measurements. Atmos Environ. 2011; 45:6267–6275.

35. Lee M, Kloog I, Chudnovsky A, Lyapustin A, Wang Y, Melly S, Coull B, Koutrakis P, Schwartz J. Spatiotemporal prediction of fine particulate matter using high-resolution satellite images in the Southeastern US 2003–2011. J Expo Sci Env Epid. 2015

36. Liu Y, Paciorek CJ, Koutrakis P. Estimating Regional Spatial and Temporal Variability of $PM_{2.5}$ Concentrations Using Satellite Data, Meteorology, and Land Use Information. Environ Health Persp. 2009; 117:886–892.

37. Li F, Ramanathan V. Winter to summer monsoon variation of aerosol optical depth over the tropical Indian Ocean. J Geophys Res Atoms (1984–2012). 2002; 107(D16):AAC 2-1–AAC 2-13.

38. Schaap M, Apituley A, Timmermans R, Koelemeijer R, Leeuw Gd. Exploring the relation between aerosol optical depth and $PM_{2.5}$ at Cabauw, the Netherlands. Atmos Chem Phys. 2009; 9(3):909–925.

39. Dubovik O, Holben B, Eck TF, Smirnov A, Kaufman YJ, King MD, Tanré D, Slutsker I. Variability of absorption and optical properties of key aerosol types observed in worldwide locations. J Atmos Sci. 2002; 59(3):590–608.

40. Hu RM, Sokhi R, Fisher B. New algorithms and their application for satellite remote sensing of surface $PM_{2.5}$ and aerosol absorption. J Aerosol Sci. 2009; 40(5):394–402.

41. Al-Saadi J, Szykman J, Pierce RB, Kittaka C, Neil D, Chu DA, Remer L, Gumley L, Prins E, Weinstock L. Improving national air quality forecasts with satellite aerosol observations. B Am Meteorol Soc. 2005; 86(9):1249–1261.

42. Bey I, Jacob DJ, Yantosca RM, Logan JA, Field BD, Fiore AM, Li Q, Liu HY, Mickley LJ, Schultz MG. Global modeling of tropospheric chemistry with assimilated meteorology: Model description and evaluation. J Geophys Res. 2001; 106:23073.

43. Byun, DW., Ching, J. Science algorithms of the EPA Models-3 community multiscale air quality (CMAQ) modeling system. United States Environmental Protection Agency; Washington, DC: 1999.

44. Bessagnet B, Hodzic A, Vautard R, Beekmann M, Cheinet S, Honoré C, Liousse C, Rouil L. Aerosol modeling with CHIMERE—preliminary evaluation at the continental scale. Atmos Environ. 2004; 38:2803–2817.

45. Jun M, Stein ML. Statistical comparison of observed and CMAQ modeled daily sulfate levels. Atmos Environ. 2004; 38:4427–4436.

46. Cordero L, Malakar N, Wu Y, Gross B, Moshary F, Ku M. Assessing satellite based $PM_{2.5}$ estimates against CMAQ model forecasts, SPIE Remote Sensing. Int Soc Opt & Polym. 2013; 8890(Oct 17th)

47. van Donkelaar A, Martin RV, Brauer M, Boys BL. Use of satellite observations for long-term exposure assessment of global concentrations of fine particulate matter. Environ Health Persp. 2015; 123(2):135.

48. Di Q, Koutrakis P, Schwartz J. A Hybrid Prediction Model for $PM_{2.5}$ Mass and Components Using a Chemical Transport Model and Land Use Regression. Atmos Environ. 2016; 131:390–399.

49. King MD, Kaufman YJ, Menzel WP, Tanre D. Remote sensing of cloud, aerosol, and water vapor properties from the Moderate Resolution Imaging Spectrometer (MODIS). IEEE T Geosci Remote. 1992; 30(1):2–27.

50. Salomonson VV, Barnes W, Maymon PW, Montgomery HE, Ostrow H. MODIS: Advanced facility instrument for studies of the Earth as a system. IEEE T Geosci Remote. 1989; 27(2):145–153.

51. Remer LA, Kaufman YJ, Tanré D, Mattoo S, Chu DA, Martins JV, Li RR, Ichoku C, Levy RC, Kleidman RG, et al. The MODIS Aerosol Algorithm, Products, and Validation. J Atmos Sci. 2005; 62:947–973.

52. Chudnovsky A, Lyapustin A, Wang Y, Schwartz J, Koutrakis P. Analyses of high resolution aerosol data from MODIS satellite: a MAIAC retrieval, southern New England, US. First International Conference on Remote Sensing and Geoinformation of the Environment. 2013; 8795(Aug 5th)

53. Lyapustin A, Martonchik J, Wang Y, Laszlo I, Korkin S. Multiangle implementation of atmospheric correction (MAIAC): 1. Radiative transfer basis and look-up tables. J Geophys Res Atoms (1984–2012). 2011; 116(D3)

54. Lyapustin A, Wang Y, Laszlo I, Kahn R, Korkin S, Remer L, Levy R, Reid J. Multiangle implementation of atmospheric correction (MAIAC): 2. Aerosol algorithm. J Geophys Res Atoms (1984–2012). 2011; 116(D3)

55. van Donkelaar A, Martin RV, Park RJ. Estimating ground-level $PM_{2.5}$ using aerosol optical depth determined from satellite remote sensing. J Geophys Res. 2006; 111

56. Di Q, Schwartz J. Using Chemical Transport Model to Fill in the Missingness of Satellite-Based AOD. Atmos Environ. In review.

57. Drury E, Jacob DJ, Wang J, Spurr RJ, Chance K. Improved algorithm for MODIS satellite retrievals of aerosol optical depths over western North America. J Geophys Res Atoms (1984–2012). 2008; 113(D16)

58. Vermote E. MOD09A1 MODIS/Terra Surface Reflectance 8-Day L3 Global 500m SIN Grid V006. NASA EOSDIS Land Processes DAAC. 2015

59. Isakov V, Touma J, Touma J, Khlystov A, Sattler M, Devanathan S, Devanathan S, Engel-Cox J, Weber S, McFarland M, et al. Estimating Fine Particulate Matter Component Concentrations and Size Distributions Using Satellite-Retrieved Fractional Aerosol Optical Depth: Part 2—A Case Study. J Air Waste Manage. 2007; 57:1360–1369.

60. Liu Y. Mapping annual mean ground-level $PM_{2.5}$ concentrations using Multiangle Imaging Spectroradiometer aerosol optical thickness over the contiguous United States. J Geophys Res. 2004; 109

61. Kalnay E, Kanamitsu M, Kistler R, Collins W, Deaven D, Gandin L, Iredell M, Saha S, White G, Woollen J, et al. The NCEP/NCAR 40-Year Reanalysis Project. B Am Meteorol Soc. 1996; 77:437–471.

62. Herman J, Bhartia P, Torres O, Hsu C, Seftor C, Celarier E. Global distribution of UV-absorbing aerosols from Nimbus 7/TOMS data. J Geophys Res. 1997; 102(16):911–16.

63. Tegen I, Werner M, Harrison S, Kohfeld K. Relative importance of climate and land use in determining present and future global soil dust emission. Geophys Res Lett. 2004; 31(5)

64. Torres O, Bhartia P, Herman J, Ahmad Z, Gleason J. Derivation of aerosol properties from satellite measurements of backscattered ultraviolet radiation: Theoretical basis. J Geophys Res Atoms (1984–2012). 1998; 103(D14):17099–17110.

65. Stein-Zweers D, Veefkind P. OMI/Aura Multi-wavelength Aerosol Optical Depth and Single Scattering Albedo Daily L3 Global 0.25×0.25 deg Lat/Lon Grid, version 003. NASA Goddard Space Flight Center. 2012

66. Torres O, Tanskanen A, Veihelmann B, Ahn C, Braak R, Bhartia PK, Veefkind P, Levelt P. Aerosols and surface UV products from Ozone Monitoring Instrument observations: An overview. J Geophys Res Atoms (1984–2012). 2007; 112(D24)

67. Kloog I, Nordio F, Coull BA, Schwartz J. Incorporating Local Land Use Regression And Satellite Aerosol Optical Depth In A Hybrid Model Of Spatiotemporal $PM_{2.5}$ Exposures In The Mid-Atlantic States. Environ Sci Technol. 2012; 46:11913–11921. [PubMed: 23013112]

68. Didan K. MOD13A2 MODIS/Terra Vegetation Indices 16-Day L3 Global 1km SIN Grid V006. NASA EOSDIS Land Processes DAAC. 2015

69. Lee H, Liu Y, Coull B, Schwartz J, Koutrakis P. A novel calibration approach of MODIS AOD data to predict $PM_{2.5}$ concentrations. Atmos Chem Phys. 2011; 11(15):7991–8002.

70. Kottek M, Grieser J, Beck C, Rudolf B, Rubel F. World map of the Köppen-Geiger climate classification updated. Meteorol Z. 2006; 15(3):259–263.

71. Bishop, CM. Neural networks for pattern recognition. Oxford university press; 1995.

72. Haykin S, Network N. A comprehensive foundation. Neural Networks. 2004; 2(2004)

73. LeCun Y, Bengio Y. Convolutional networks for images, speech, and time series. The handbook of brain theory and neural networks. 1995; 3361(10)

74. Sharkey TD, Wiberley AE, Donohue AR. Isoprene emission from plants: why and how. Ann Bot. 2008; 101(1):5–18. [PubMed: 17921528]

75. Claeys M, Graham B, Vas G, Wang W, Vermeylen R, Pashynska V, Cafmeyer J, Guyon P, Andreae MO, Artaxo P. Formation of secondary organic aerosols through photooxidation of isoprene. Science. 2004; 303(5661):1173–1176. [PubMed: 14976309]

76. Park RJ, Jacob DJ, Field BD, Yantosca RM, Chin M. Natural and transboundary pollution influences on sulfate-nitrate-ammonium aerosols in the United States: Implications for policy. J Geophys Res Atoms (1984–2012). 2004; 109(D15)

77. Sharkey TD, Singsaas EL, Vanderveer PJ, Geron C. Field measurements of isoprene emission from trees in response to temperature and light. Tree Physiol. 1996; 16(7):649–654. [PubMed: 14871703]

78. Geron C, Harley P, Guenther A. Isoprene emission capacity for US tree species. Atmos Environ. 2001; 35(19):3341–3352.

79. Franklin M, Koutrakis P, Schwartz P. The role of particle composition on the association between $PM_{2.5}$ and mortality. Epidemiology. 2008; 19(5):680–9. [PubMed: 18714438]

80. Dai L, Zanobetti A, Koutrakis P, Schwartz JD. Associations of fine particulate matter species with mortality in the United States: a multicity time-series analysis. Environ Health Persp. 2014; 122:837.
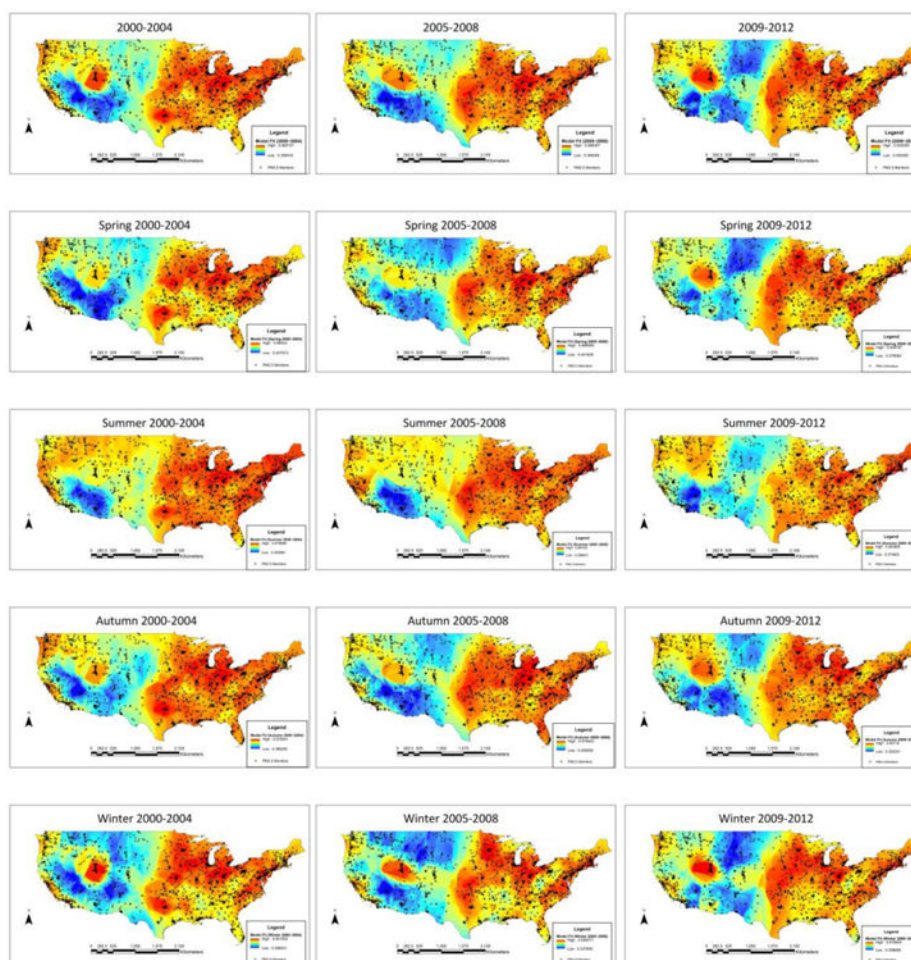
Figure 1. Model performance in the continental United States

We calculated total R^2 between monitored and predicted $PM_{2.5}$ for each monitoring site and interpolated R^2 to places without monitors using Kriging interpolation. Spring was defined as March to May; summer was defined as June to August; autumn was defined as September to November; winter was from December to February of the next year (same below). The red color stands for high R^2, and the blue color stands for low R^2.
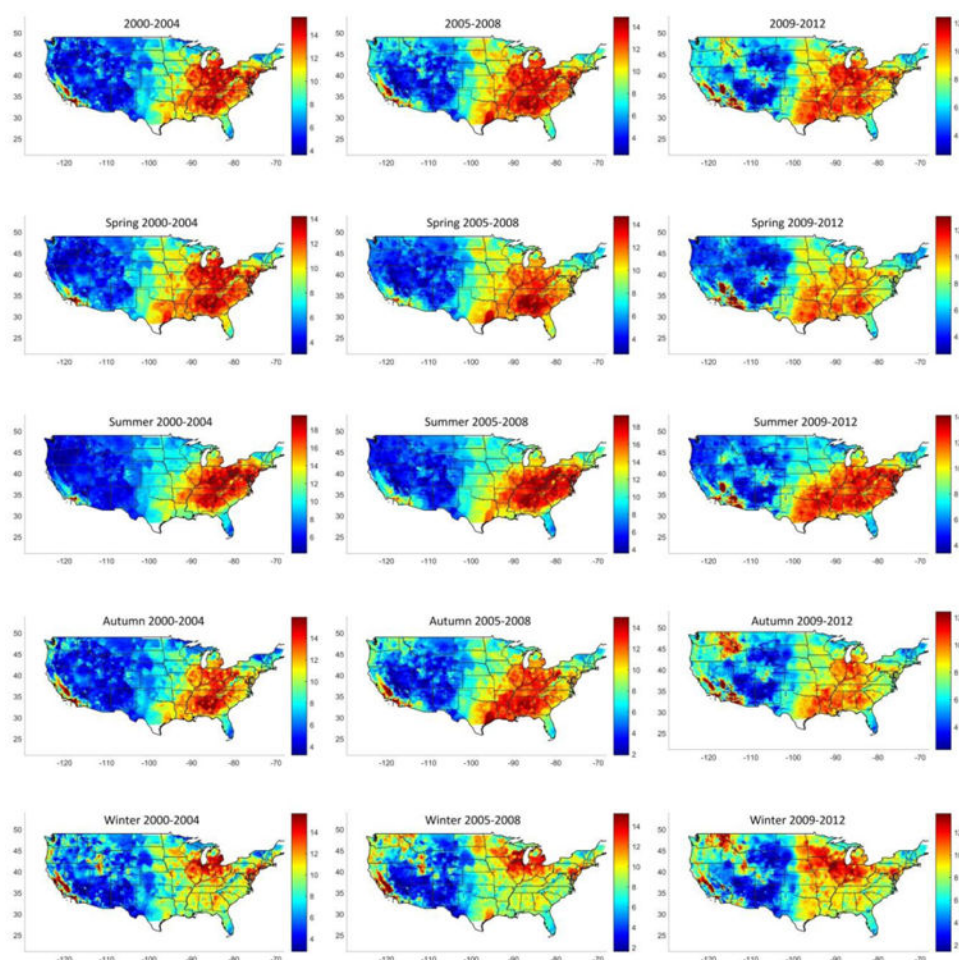
Figure 2. Spatial distribution of predicted PM$_{2.5}$
Trained neural network predicted daily total PM$_{2.5}$ concentration at 1 km×1 km grid cell in the study area. The red color stands for high concentrations, and the blue color stands for low concentrations.
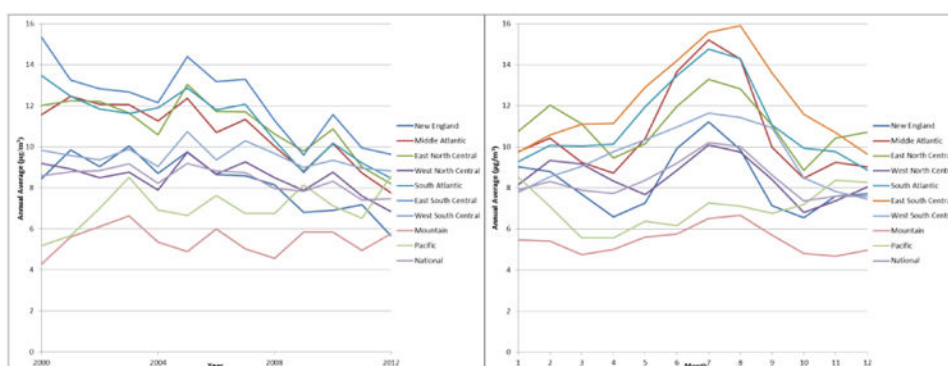
Figure 3. Annual means by month of year and by region
Annual averages were computed by averaging all predicted PM$_{2.5}$ values at 1 km×1 km grid cells in that region or in that month.
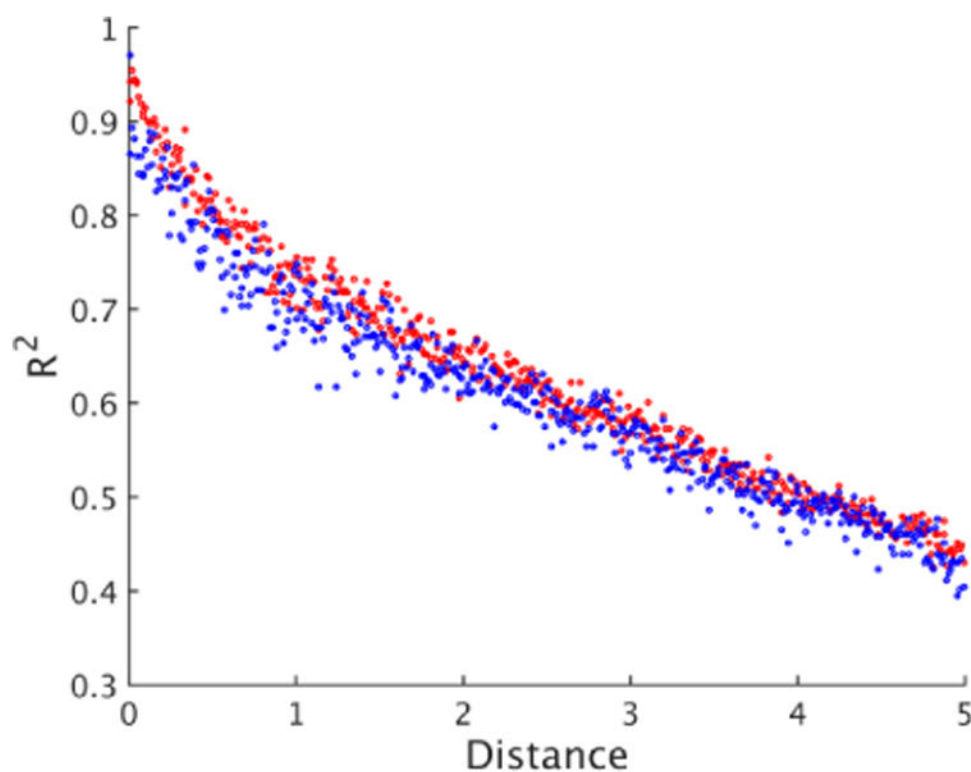
Figure 4. Relationship between correlation and distance between any two monitor sites
For 1,928 monitoring sites in the study area, we computed the correlation of $PM_{2.5}$ measurements and distance (in degree) between any two monitoring site pairs and plotted the between-site correlation versus between-site distance (red dots). We repeated the same process for predicted $PM_{2.5}$ and plotted the correlation of predicted $PM_{2.5}$ and monitored $PM_{2.5}$ between two site pairs versus distance (blue dots). This figure is for year 2012.
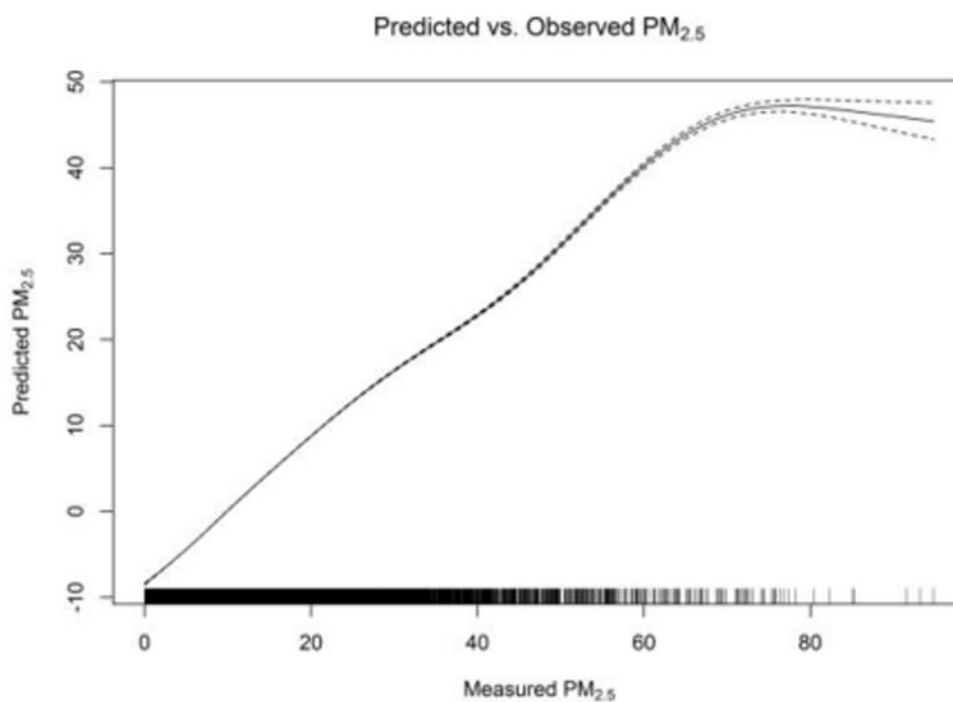
Figure 5. Relationship between measured PM$_{2.5}$ and predicted PM$_{2.5}$
We fit a penalized spline between measured PM$_{2.5}$ and predicted PM$_{2.5}$ without specifying degree of freedom. This figure is for year 2009.

Table 1

Cross-validated R^2 for the whole study area

Year	Total R^2	RMSE	Spatial R^2	RMSE	Temporal R^2	RMSE	Bias	Slope
2000	0.86	3.35	0.85	1.52	0.85	3.07	0.22	1.01
2001	0.84	3.58	0.86	1.40	0.83	3.35	0.22	1.01
2002	0.88	2.99	0.88	1.24	0.88	2.75	0.25	1.00
2003	0.88	2.80	0.87	1.21	0.88	2.57	0.23	1.00
2004	0.88	2.69	0.79	1.50	0.88	2.45	0.22	1.00
2005	0.88	2.94	0.84	1.45	0.89	2.66	0.27	1.00
2006	0.86	2.77	0.80	1.34	0.86	2.50	0.25	1.00
2007	0.87	2.95	0.83	1.31	0.87	2.72	0.21	1.00
2008	0.85	2.64	0.79	1.26	0.86	2.40	0.19	1.00
2009	0.82	2.73	0.81	1.09	0.82	2.54	0.21	1.00
2010	0.81	2.85	0.84	1.21	0.81	2.60	0.51	0.98
2011	0.81	2.83	0.81	1.11	0.81	2.60	0.38	0.99
2012	0.74	3.15	0.78	1.16	0.74	2.92	0.32	1.00
Mean	0.84	2.94	0.83	1.29	0.84	2.70	0.27	1.00